ELSEVIER

Journal of Nuclear Materials 253 (1998) 156–166

journal of nuclear materials

Electrical conductivity change in single crystal Al_2O_3 and MgO under neutron and gamma-ray irradiation

Takaaki Tanifuji *, Yoshio Katano, Tetsuya Nakazawa, Kenji Noda

Japan Atomic Energy Research Institute, Tokai-mura, Naka-gun, Ibaraki-ken 319-11, Japan

Abstract

In situ electrical conductivity measurements under reactor and gamma-ray irradiation were carried out for Al_2O_3 and MgO specimens using JRR-3 and a ^{60}Co gamma-ray irradiation facility at JAERI. The specimens were irradiated in the temperature range 573 to 723 K for two cycles (about 0.2 dpa) with an applied dc electric field of 100 V/mm. The conductivity level evaluated after the shutdown of the reactor was substantially smaller than those during the reactor operation. Thus, it was considered that radiation induced electrical degradation (RIED) did not occur or was a negligibly small level, up to 0.2 dpa for Al_2O_3 and MgO specimens. The conductivity of the Al_2O_3 specimen evaluated at various reactor powers in JRR-3 was consistent with that measured under the ^{60}Co gamma-ray irradiation and was in fairly good agreement with the other radiation induced conductivity (RIC) data of high-purity Al_2O_3. © 1998 Elsevier Science B.V.

1. Introduction

Many ceramic materials will be used as electrical insulator materials for various diagnostics components, the first wall current break, reduction of electromagnetic force to various in-vessel components, the radio frequency (rf) heating windows, etc. in D–T fusion reactors. During operation of the fusion reactors, radiation-induced conductivity (RIC) takes place in the ceramic insulators by exciting electrons from the valence band to the conduction band with high energy neutrons and gamma-rays. The RIC due to X-ray, gamma-ray, electron, proton and fission neutron irradiation has been measured for ceramic insulator materials such as Al_2O_3, MgO, etc. [1–7]. Recently, the RIC due to 14 MeV neutrons which characterize fusion reactor neutron irradiation environment was also investigated for Al_2O_3 using the Fusion Neutronics Source (FNS) at the Japan Atomic Energy Research Institute (JAERI) [8]. By comparing the RIC data due to X-ray, gamma-ray, electron, proton, fission neutron and 14 MeV neutron irradiations with each other, it was suggested that the RIC as a function of ionization dose rate depended on impurity and radiation damage levels but not on the difference of the type of irradiation.

Although the RIC is an instantaneous effect under irradiation, a severe permanent increase in electrical conductivity of ceramic insulators irradiated under applied electric filed greater than 20 V/mm, i.e. radiation induced electrical degradation (RIED), has been reported [5,9–14]. The magnitude of RIED has been measured to exceed 10^{-4} S/m in some studies, which is an unacceptable level of degradation of electrical insulation for most fusion insulator applications and, therefore, the RIED phenomenon is a more serious technological issue than the RIC. In the above-mentioned studies, the RIED was found to occur in the temperature range 473 to 823 K with an even rather low damage level of 10^{-5} to 0.1 dpa (for instance, RIED of Al_2O_3 occurred around 750 K at about 10^{-5}, 10^{-3} and 10^{-2} dpa for electron, proton and fission neutron irradiation, respectively). On the other hand, it has been reported that the RIED does not occur for some examined Al_2O_3 in the conditions of irradiation, temperature and applied electrical field in which the RIED was found in the above-mentioned studies [15–17].

The physical process responsible for the RIED still remains uncertain. Aluminum metal colloid, F^+ centers, impurity levels, dislocations and precipitation of different phases have been considered to be associated with the appearance of RIED as bulk effects [18]. On the other

* Corresponding author. Tel.: +81-29 282 5435; fax: +81-29 282 5460; e-mail: tanifuji@maico.tokai.jaeri.go.jp

PII S0022-3115(97)00310-3

hand, the large degradation of electrical insulation recognized as RIED was assumed to occur due to surface leakage current arising from surface degradation such as contamination, microcracking, etc. in some recent studies [19].

In this investigation, in situ electrical conductivity measurements of Al_2O_3 and MgO under fission reactor and gamma-ray irradiation were carried out using the JRR-3 water-cooled fission reactor and a ^{60}Co gamma-ray irradiation facility at Japan Atomic Energy Research Institute (JAERI), in order to obtain knowledge on the RIC and RIED of the materials to understand the phenomena and fusion engineering application.

2. Experimental

2.1. Specimens

High purity α-Al_2O_3 single crystal (Kyocera SA 100, purity; 99.999%) and MgO single crystal (Tateho T98) disks of about 8.5 mm in diameter and about 0.2 mm in thickness were used and the surface orientations of the α-Al_2O_3 and MgO disk specimens were (0001) and {100}, respectively. The α-Al_2O_3 and MgO disk specimens were annealed at 1270 K for 4 and 6 h in air and flowing oxygen gas, respectively. Three electrodes on the top (low side) and the bottom (high side) of each specimen were made by depositing a thin titanium layer (thickness; 15 nm) and subsequently a platinum layer (thickness; 200 nm) using the vacuum sputter-deposition method. The configuration of the three electrodes is shown in Fig. 1. The low-side center electrode was 3.5 mm in diameter and had a guard ring of 5.5/7.5 mm in inner/outer diameter. The high-side electrode was a single electrode of 7.5 mm diameter.

2.2. Irradiation capsule for in situ measurement of electrical conductivity in JRR-3 and measurement system

An irradiation capsule for in situ electrical conductivity measurements contains two specimen holders for electrical conductivity measurements of the Al_2O_3 and MgO specimens. Fig. 2 shows schematic illustrations of the irradiation capsule and the specimen holder. The specimen holder consists of two cylindrical high-purity Al_2O_3 sintered blocks (an upper block: 21.8 mm in diameter and 6.5 mm in height; and a lower block: 21.8 mm in diameter and 10 mm in height). Lead pins made of stainless steel (SUS 304) are attached to the upper block for the center electrode and the guard ring and to the lower block for the single electrode. The specimen is set between the upper and lower blocks by tightening up three screws. The lead pin of the lower block which bears spring-action allows good electrical contact between the lead pins and the electrodes.

The two specimen holders mentioned above were set in an Al_2O_3 sintered sleeve contained in the irradiation cap-

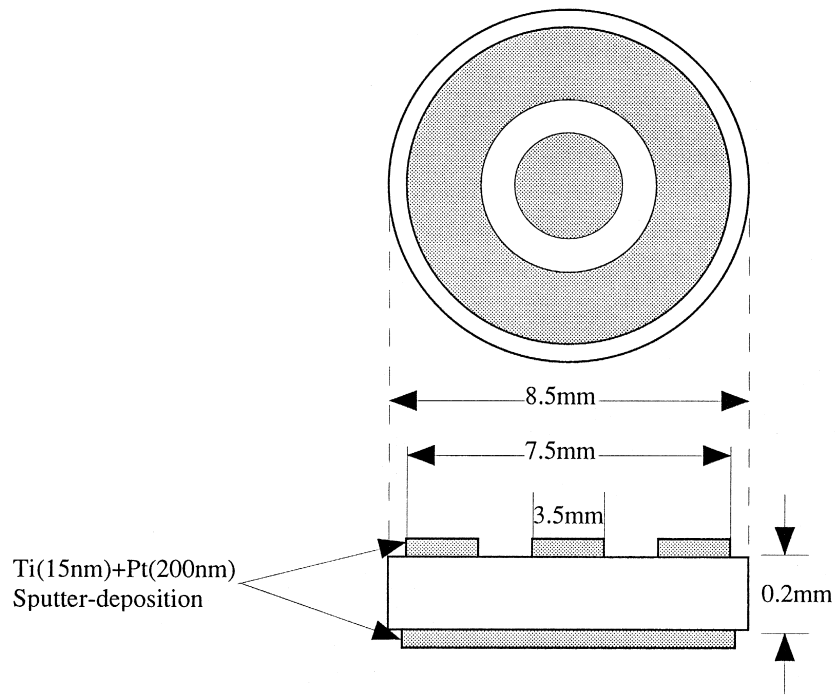

Fig. 1. Configuration of the three electrodes on the specimen.

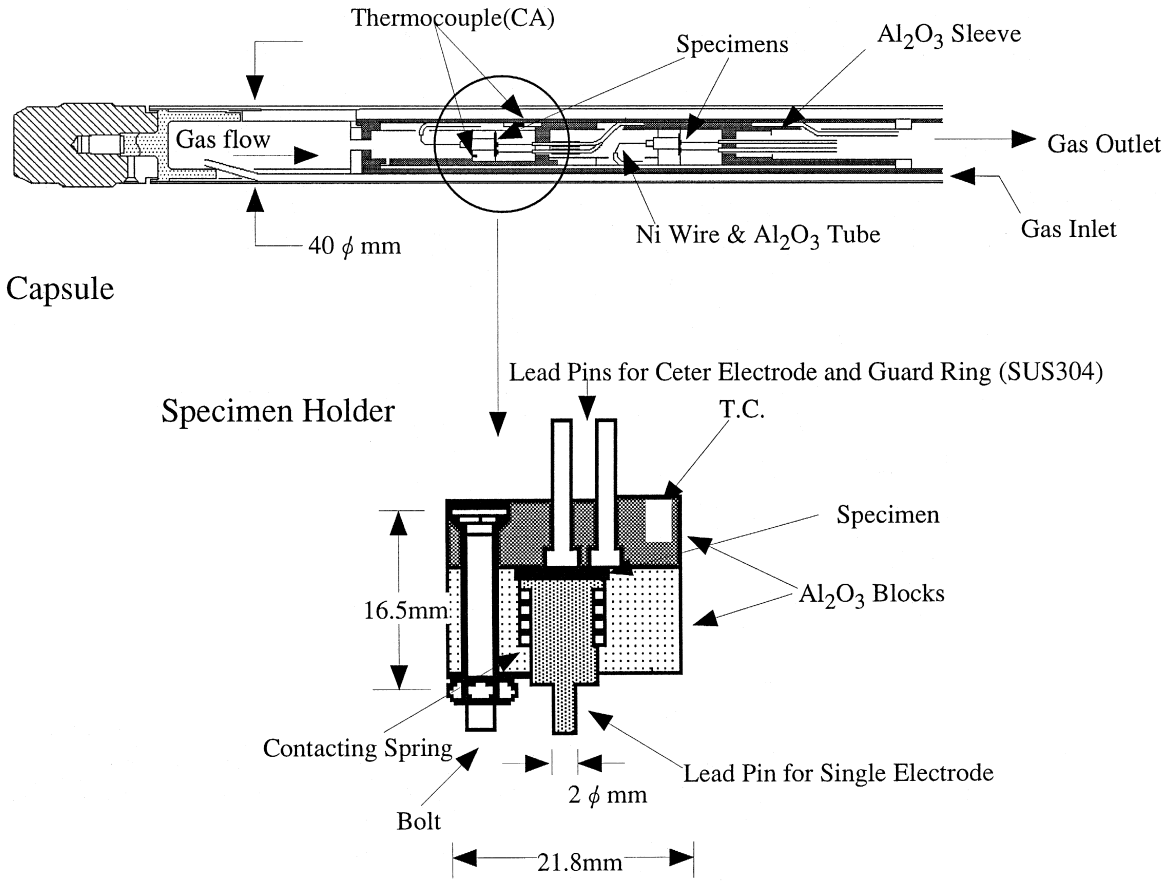

Fig. 2. Schematic illustrations of irradiation capsule and specimen holder.

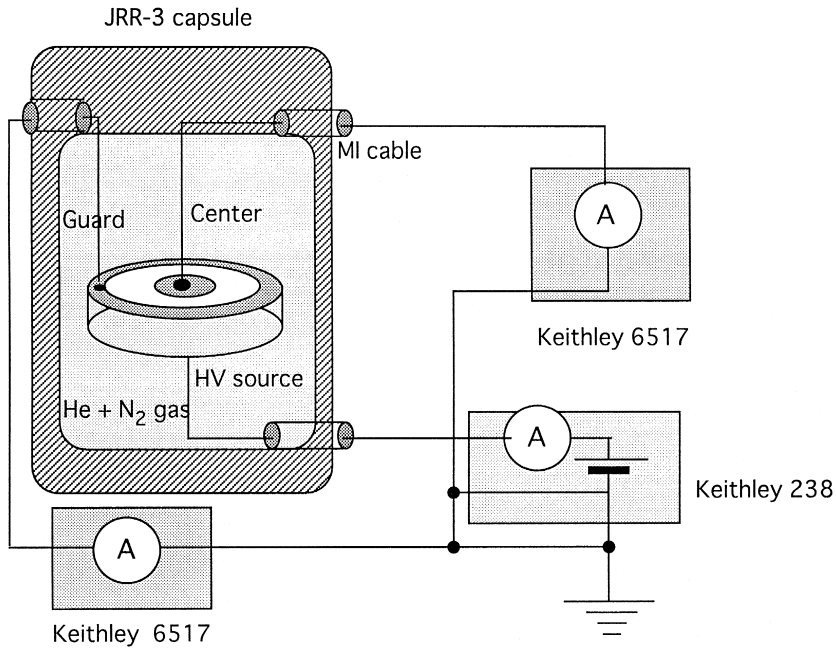

Fig. 3. Electrical diagram of measurement system.

sule. The lead wires of the lead pins for the center electrode and the high side single electrode were Ni wires (diameter 0.5 mm) covered with high-purity Al_2O_3 sintered tubes, which were connected to 1.0 mm outer diameter stainless steel sheathed, mineral insulated cable (MI cable; Thermocoax cable 1ZsAC). For the lead wire for the lead pin of the guard ring, the Ni wire, which was connected to the 1.6 mm diameter stainless steel sheathed chromel–alumel thermocouple cable, was attached. The connections between the Ni wire and the MI cables or the thermocouple wires were located at the border of the reactor core, at which the ionization dose rate is considered to be much lower than that at the specimen holder position. The stainless steel sheathed chromel–alumel thermocouple cable was embedded in each specimen holder to measure the correct temperature. The atmosphere in the irradiation capsule was a mixture of flowing He and N_2 gas. The temperature of the specimen holders during irradiation was controlled by changing the He/N_2 ratio of the mixture gas.

The electrical diagram of the measurement system is shown in Fig. 3. A dc voltage of 20 V (100 V/mm) was applied to the specimen by a Keithley 238 Source Measure Unit. The high voltage (HV) source current was measured with the same apparatus (includes the current through the bulk and surface of the specimen, as well as the leakage current due to photoelectrons through the ionized gas atmosphere, etc). On the other hand, the center current (the current through the center electrode and corresponding Ni/MI cable lead wires) and the guard current (the current through the guard ring and Ni wire/chromel–alumel thermocouple lead wires) were each measured by a high-resistance electrometer. Continuous measurements of center, guard and HV source currents for the Al_2O_3 and the MgO specimens were simultaneously measured by two sets of measurement systems. The bulk conductivity of the specimen was measured using the procedure described in ASTM 257-91, standard test method for dc resistance or conductance of insulating materials.

2.3. In situ electrical conductivity measurement system under gamma-ray irradiation

The in situ electrical conductivity measurement chamber used for the gamma-ray irradiation and the associated conductivity measurement system have been reported elsewhere [20]. A specimen holder attached to a heater was contained in a vacuum chamber of which a pressure of $< 10^{-5}$ Pa can be attained by a turbo molecular pump. The specimen temperature can be elevated up to 1370 K using the heater. The electrical conductivity of the sample was evaluated by the three-terminal dc method which was essentially similar to that in the case of in situ experiment using JRR-3. The center current and the HV source current were measured at an applied voltage of dc 20 V by using the same equipment. The guard current was not measured.

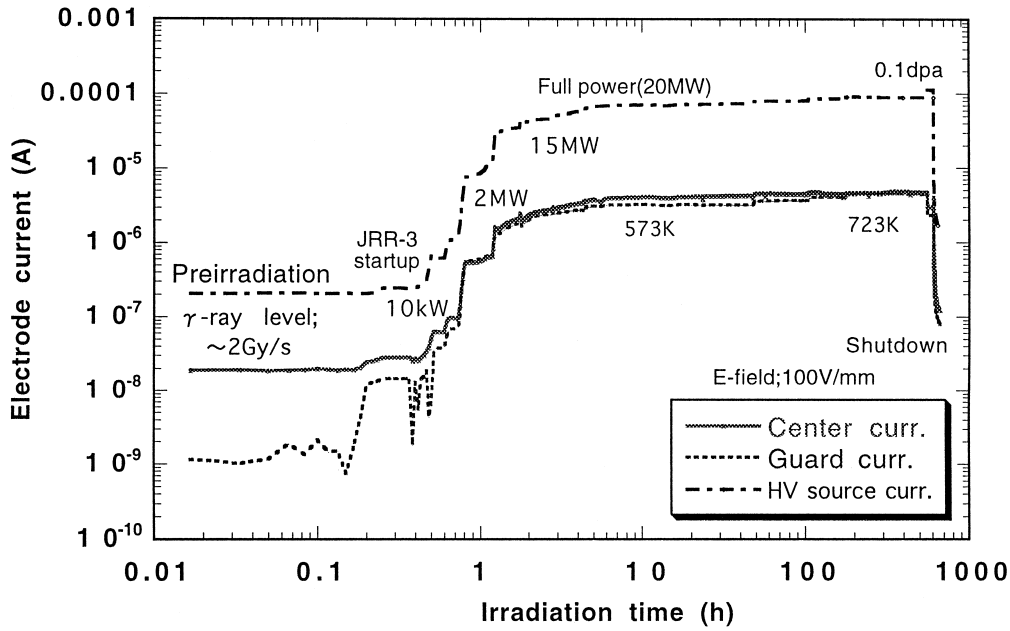

Fig. 4. Behavior of the center, the guard and the HV source currents for Al_2O_3 specimen in the first irradiation cycle (20 V applied to HV cable).

2.4. In situ electrical conductivity measurements

The center, the guard and the HV source currents was measured with an applied electric field of 100 V/mm in JRR-3 before, during and after operation of the reactor using the irradiation capsule and the measurement system mentioned previously. The thermal and fast neutron fluxes in JRR-3 under full-power operation were 2×10^{18} and 0.5×10^{18} n/m^2 s ($E > 0.1$ MeV). The gamma-ray dose level at the full reactor power can be evaluated to be about 3.4 kGy/s (for Al_2O_3) from gamma heating rate for iron. On the other hand, the gamma-ray dose level after the shutdown of the reactor is very roughly estimated to be 3 Gy/s or smaller. Irradiation for two reactor cycles was carried out. The total thermal and fast neutron fluences were 7.6×10^{24} and 1.9×10^{24} n/m^2, respectively, and this dose level corresponds to about 0.2 dpa. The irradiation temperature at the full reactor power was varied in the range 570 to 720 K by changing the He/N_2 ratio of the flowing mixture gas (average gas flow rate; 2 to 2.5 ml/s).

The electrical conductivity of an Al_2O_3 specimen under gamma-ray irradiation was measured with an applied electric field of 100 V/mm in the ^{60}Co gamma-ray irradiation facility. The dose rate of the gamma ray (1.17 and 1.33 MeV) was 5 Gy/s and a total dose of 1.4×10^5 Gy was attained. The irradiation temperature was 570 K and the atmosphere was vacuum better than 10^{-5} Pa.

3. Results

3.1. Electrical conductivity of Al_2O_3 during and after reactor irradiation

The apparent electrical conductivity at room temperature was in the order of 10^{-13} S/m for the Al_2O_3 and the MgO specimens before the capsule installation in JRR-3. Installing the capsule in JRR-3 (BR-2 irradiation position), the center, the guard and the HV source currents increased due to the residual gamma-ray ionization level (3 Gy/s or smaller) before the reactor operation start. Fig. 4 shows the behavior of the center, the guard and the HV source currents for the Al_2O_3 specimen in the first irradiation cycle. The center, the guard and the HV source currents were 2×10^{-8}, 10^{-9} and 2×10^{-7} A (the electrical conductivity of the specimen calculated from the center current: 1.1×10^{-8} S/m) before the reactor operation start. The currents increased with the reactor power and the temperature of the specimen was also raised with the power. The center, the guard and the HV source currents of 4×10^{-6}, 3×10^{-6} and 7×10^{-5} A (the electrical conductivity of the specimen: 2.2×10^{-6} S/m) were attained at the full reactor power (20 MW) for the Al_2O_3 specimen at 573 K. Fig. 5 shows the center current, the guard and the HV source currents for the Al_2O_3 specimen in the first (#08-02 cycle) and the second (#08-03 cycle) irradiation cycles versus the irradiation time. In the first

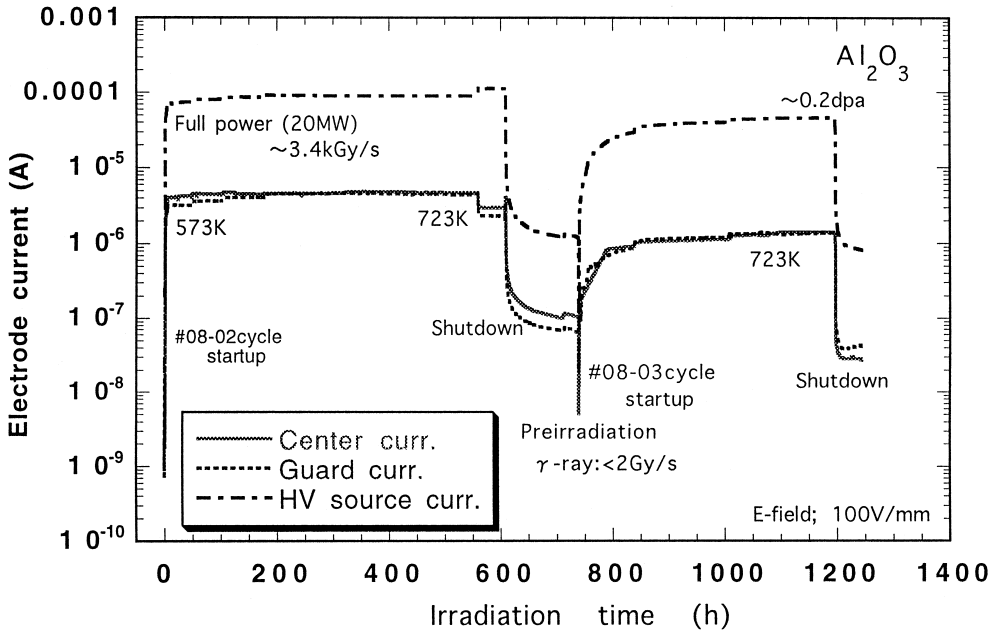

Fig. 5. The center current, the guard and the HV source currents for the Al_2O_3 specimen in the first (#08-02 cycle) and the second (#08-03 cycle) irradiation cycles versus the irradiation time (20 V applied to HV cable).

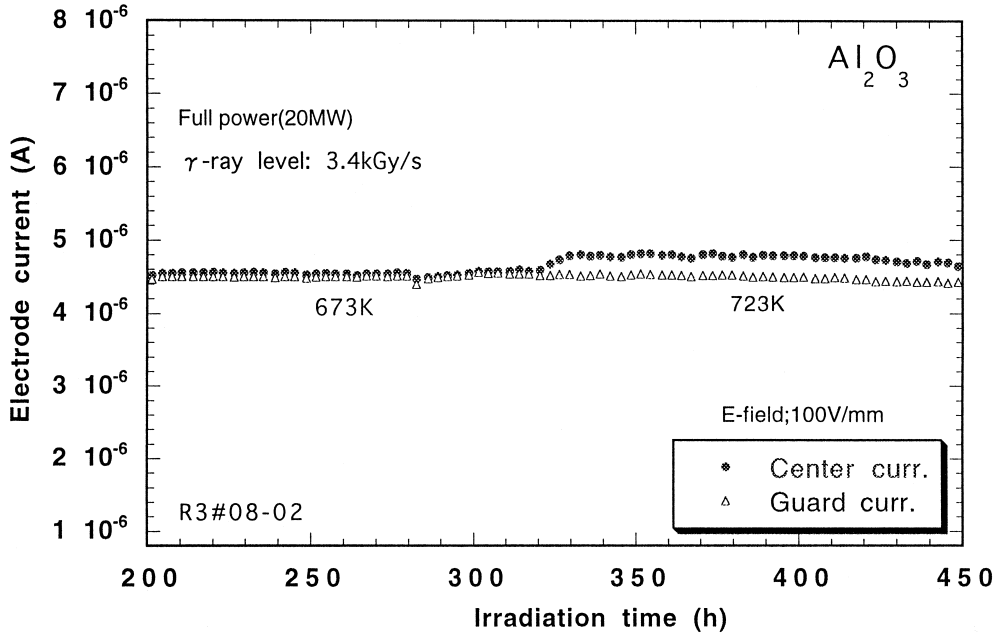

Fig. 6. Relationship between the center and the guard currents and the irradiation time for the Al_2O_3 specimen in the first irradiation cycle (20 V applied to HV cable).

irradiation cycle, the temperature of the specimens were changed into 623, 673 and 723 K after the irradiation at 573 K by changing He/N_2 ratio of the flowing mixture gas. The center, the guard and the HV source currents changed with the temperature of the specimens only slightly. The HV source current was about 20 times as

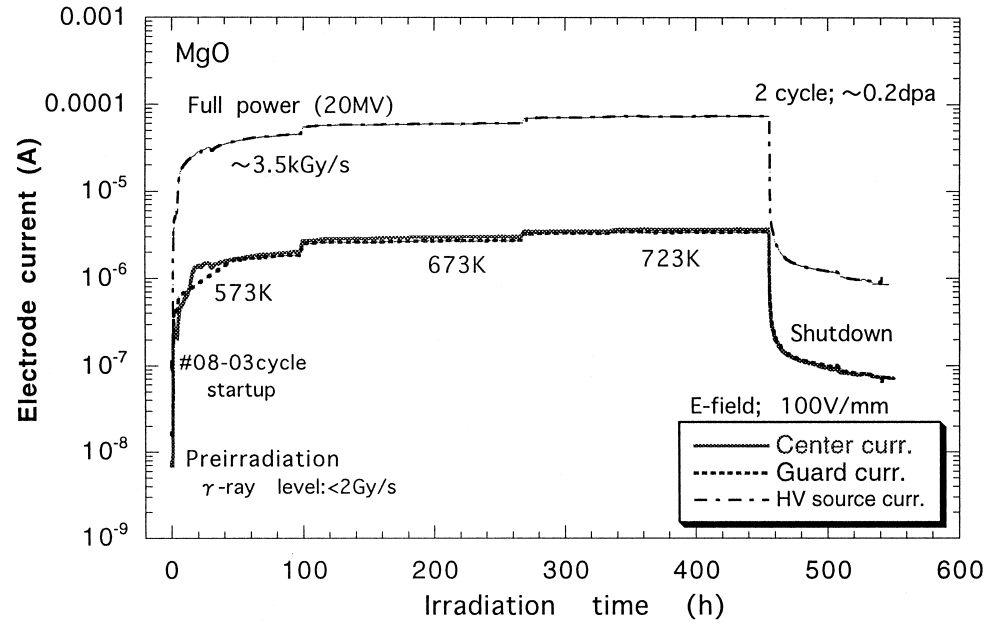

Fig. 7. The center, the guard and the HV source currents for the MgO specimen in the second (#08-03 cycle) cycles versus the irradiation time (20 V applied to HV cable).

large as the center and the guard currents. At the reactor shutdown of the first irradiation cycle, substantial decrease of these currents took place rapidly. The current then gradually decreased with time because of decay of the gamma-ray level at the specimen position, and about 10^{-7}, 7×10^{-8} and 10^{-6} A were attained for the center, the guard and the HV source current 140 h after shutdown. Further decrease of the current level took place between the first and the second irradiation cycles and it can be attributed to further decay of the gamma-ray level. The atmosphere of mixture of He and N_2 gas was maintained during the period between the first cycle and the second cycle (102 days) to avoid contamination of specimens and the other materials inside the irradiation capsule due to moisture in the air. Just prior to the reactor start in the second irradiation cycle (gamma-ray dose rate level; 3 Gy/s or smaller), the center current was about 5×10^{-9} A and this corresponds to an electrical conductivity of 3×10^{-9} S/m. These values are smaller than those before the reactor operation start in the first irradiation cycle.

After the start of the second irradiation cycle, the center, the guard and the HV source currents increased again with the reactor power as well as the temperature of the specimen. At the full reactor power, 9×10^{-7}, 8×10^{-7} and 3×10^{-5} A were attained for the center, the guard and the HV source currents at 573 K, respectively (The electrical conductivity of the specimen at 573 K: 5×10^{-7} S/m). Then, the temperature of the specimen was raised up to 723 K stepwise (i.e. 573, 673 and 723 K). The measured currents increased slightly with the temperature of the specimen. The current values measured during the second irradiation cycle were smaller than those in the first irradiation cycle. They decreased rapidly at the shutdown of the reactor in the second irradiation cycle too. The current levels measured after the shutdown were also smaller than those in the first irradiation cycle.

The relationship between the center and the guard currents and the irradiation time in the first irradiation cycle, which was shown in Fig. 5, is enlarged in Fig. 6. It is found in Fig. 6 that scattering of the measurement data is small and that the center current at 673 and 723 K was constant or decreased with the irradiation time, i.e. irradiation fluence, slightly.

3.2. Electrical conductivity of MgO during and after reactor irradiation

The behavior of the measurement currents and the electrical conductivity of the MgO specimen was similar to the case of the Al_2O_3 specimen: The measured electrical conductivity before the capsule installation in JRR-3 (on the order of 10^{-13} S/m) increased by the installation, and the center, the guard and the HV source currents increased with the reactor power as well as the temperature of the specimen. Fig. 7 shows the center, the guard and the HV source currents for the MgO specimen in the second (#08-03 cycle) cycle versus the irradiation time. After the reactor start in the second irradiation cycle, the center, the guard and the HV source currents of 2×10^{-6}, 2×10^{-6} and 5×10^{-5} A (the electrical conductivity of the specimen: 1.1×10^{-6} S/m) were attained at the full reactor power for the MgO specimen at 573 K. After that, the

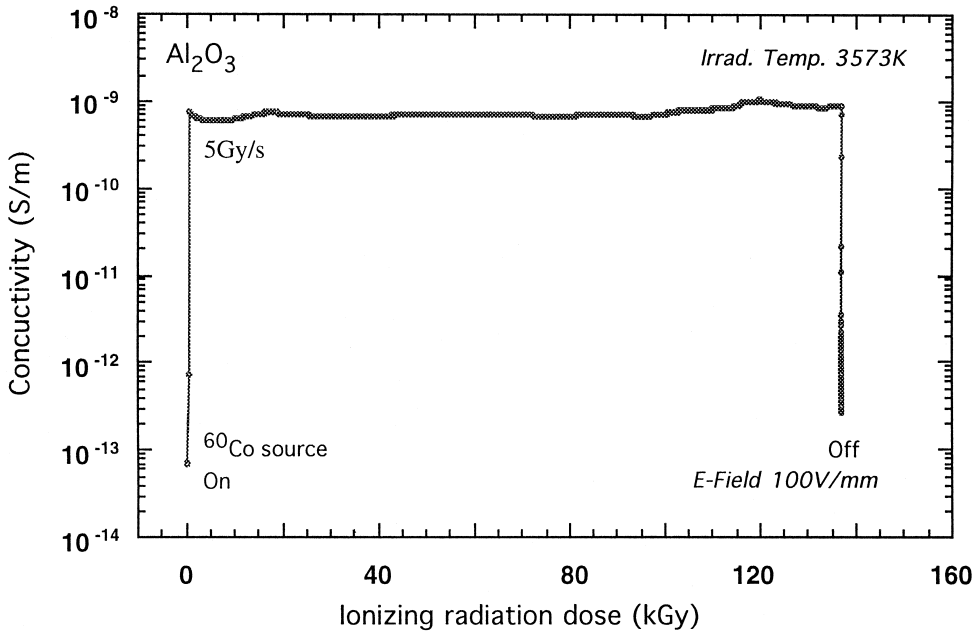

Fig. 8. Behavior of the electrical conductivity of the Al_2O_3 specimen at 573 K during the gamma-ray irradiation at the dose rate of 5 Gy/s.

temperature dependence of the measured currents was investigated by raising up the temperature of the specimen to 673 and 723 K. The currents increased slightly with the increasing temperature, similar to that of the Al_2O_3 specimens. The HV source current was much larger than the center and the guard currents and the ratio between HV source current and center or guard current was similar to the case of the Al_2O_3 specimens. A substantial decrease of the currents at the reactor shutdown was followed by a gradual decrease. The center current after the shutdown in the second irradiation cycle was about 7×10^{-8} A, which was larger than that just before the reactor operation start of the second cycle (7×10^{-9} A). However, the center current may be considered to decrease to the level similar to the value just before the reactor operation start after several tens to a hundred days, since further decay of the gamma-ray level near the specimen occurs as shown in Fig. 5. For the Al_2O_3 specimen, the center current decreased slightly with the irradiation fluence, as mentioned previously. In contrast with the Al_2O_3 specimen, a slight increase of the center current was observed for the MgO specimen.

For the first irradiation cycle, behavior of the center and the HV source currents, which was essentially similar to that in the second irradiation cycle, was observed, although the guard current was not measured (the guard lead wire was directly connected to the ground terminal of Keithley 238 Source Measure Unit during first reactor cycle.).

3.3. Electrical conductivity of Al_2O_3 during gamma-ray irradiation

Fig. 8 shows typical behavior of the electrical conductivity of the Al_2O_3 specimen at 573 K during ^{60}Co gamma-ray irradiation at the dose rate of 5 Gy/s. The gamma-ray dose level of 1.4×10^5 Gy was attained. At the irradiation start, the conductivity of the specimen (conductivity before the irradiation; around 10^{-13} S/m) increased rapidly due to RIC, and the RIC level of about 8×10^{-10} S/m was attained. The RIC level was maintained with slight fluctuation up to the end of the gamma-ray irradiation of the dose level of 1.4×10^5 Gy. At the end of the irradiation, the conductivity decreased to reach the conductivity level before the irradiation.

4. Discussion

In the in situ irradiation test for electrical conductivity measurements of Al_2O_3 and MgO using JRR-3, the HV source current was much larger than the center and guard currents. This large HV source current arises from combination of electrical conduction due to photoelectrons through gas atmosphere, RIC leakage in the Al_2O_3 tubes covering the Ni wire and the MI cable, and surface leakage between high side single electrode and the guard rind and between the center electrode and the guard ring. Similar phenomenon was also observed for the recent study of Farnum et al. In which the electrical conductivity of Al_2O_3 and MI cables under and after reactor irradiation was evaluated using JMTR at JAERI [17]. In their study, the large current was considered to be predominantly attributed to ejection of photoelectrons from the capsule walls that were attracted to the unshielded electrode wires thorough ionized gas atmosphere. Such photoelectrons were considered to result in the non-ohmic behavior of not only the HV source current but also the low-side center current. Changing the measurement voltage from positive voltage to negative voltage led to a significant decrease of the current, which was attributed to the ejection of photoelectrons and produced an approximately ohmic behavior of the measured currents in their study. Such suppression of the non-ohmic behavior for negative voltages was also observed in the recent work using HFIR [22].

In the present study, the center, the guard and the HV source currents was measured as a function of the applied voltage during irradiation at the full power. Although the measured current increased with the increase of applied voltage in case of the positive voltage, the gradient of relationship between the current and the voltage decreased with increase of the applied voltage. Such non-ohmic behavior was more prominent for the HV source current than for the center and the guard currents. On the other hand, the non-ohmic behavior was considerably suppressed in case of the negative voltage. This behavior is essentially similar to those observed in the study of Farnum et al. and the recent work using HFIR [17,22]. Surface leakage resistance between the center electrode and the guard ring before the reactor operation start. The measured current at the applied voltage of 20 V was about 8×10^{-9} A for both the Al_2O_3 and the MgO specimens and this corresponded to surface resistance of about 10^{10} Ω. However, in this measurement condition, not only surface leakage current but also RIC in bulk due to the gamma dose rate level before the reactor operation start contribute the measured current. This means that the surface resistance is larger than 10^{10} Ω. Furthermore, potential difference between the center electrode and the guard ring was smaller than 20 V, when the center, the guard and the HV source currents were measured in the reactor. It is, therefore, considered that the influence of surface leakage current on the measurement of center current is very small.

The Ni lead wires were covered by Al_2O_3 tubes, which was not a perfect shield to gas atmosphere in the capsule, was used and a positive voltage (20 V) was applied to the specimen. It is, therefore, possible that leakage currents due to photoelectrons through ionized gas atmosphere contributed to the increase of the HV source, the center and the guard currents. The contribution of the leak current to the HV source current is very large, since a huge number of photoelectrons ejected from the capsule walls

would be mainly attracted to the lead wire of the high side single electrode. On the other hand, the influence due to the leak current for the center and guard currents should be small in comparison with the case of the HV source current, because the electrical potential of the center electrode and guard ring lead wires is nearly equal to the ground and the number of photoelectrons ejected from these lead wires may not be so large in comparison with that from the capsule walls. Such electrical potential of the center electrode lead wire and the MI cable should also lead to a smaller contribution of the RIC leakage in the Al_2O_3 tubes covering the Ni wire and the MI cable to the center current in comparison with the case of the HV source current, for which the lead wire and the MI cable have the electrical potential difference of 20 V between ground and them.

The center current for the Al_2O_3 specimen decreased substantially at the shutdown of the first and the second irradiation cycles, to become 1/40 to 1/75 of the values just before the shutdown, which was close to the value before the irradiation. Furthermore, the center current just before the second irradiation cycle, at which the gamma-ray level was sufficiently decayed, was smaller than the center current value just before the first irradiation cycle. These suggest that RIED does not occur or is negligibly small for the Al_2O_3 specimen irradiated up to the end of the second irradiation cycle (0.2 dpa) at temperatures in the range 573 to 723 K. In addition, the center current at the examined temperature remained constant or decreased slightly with the irradiation fluence. This seems to support the above-mentioned evidence that RIED did not occur or is negligible small in the Al_2O_3 specimen up to 0.2 dpa. However, post-irradiation measurements of the electrical conductivity (without ionizing radiation) versus temperature up to 723 K are needed to fully confirm the absence of any RIED.

For the MgO specimen, a substantial decrease of the center current was also observed at the shutdown of the first and the second irradiation cycle. The influence of the leak currents due to photoelectrons through the ionized gas atmosphere, etc. is considered to be small at the reactor shutdown, as mentioned in the case of the Al_2O_3 specimen. It is considered from the experimental data that RIED does not take place or is negligibly small for the MgO specimen irradiated up to 0.2 dpa at the temperature in the range 573 to 723 K as well as the Al_2O_3 specimen.

It is seen in Figs. 4 and 5 that the center current values are nearly the same as the guard current values at the full reactor power, although these values do not necessarily the same before the reactor operation start and after the reactor shutdown. The nearly same values for the center and the guard currents may be predominantly attributed to the leakage currents due to photoelectrons through gas atmosphere and RIC in the insulator of lead wires for the center electrode and the guard ring.

The gamma-ray dose rate in JRR-3 is estimated to be about 3.4 kGy/s at the full power for the Al_2O_3 and MgO specimens from a known gamma heating rate of iron (3.2 W/g). On the other hand, the ionization dose rate of neutrons may be estimated to be in the order of 10 Gy/s,

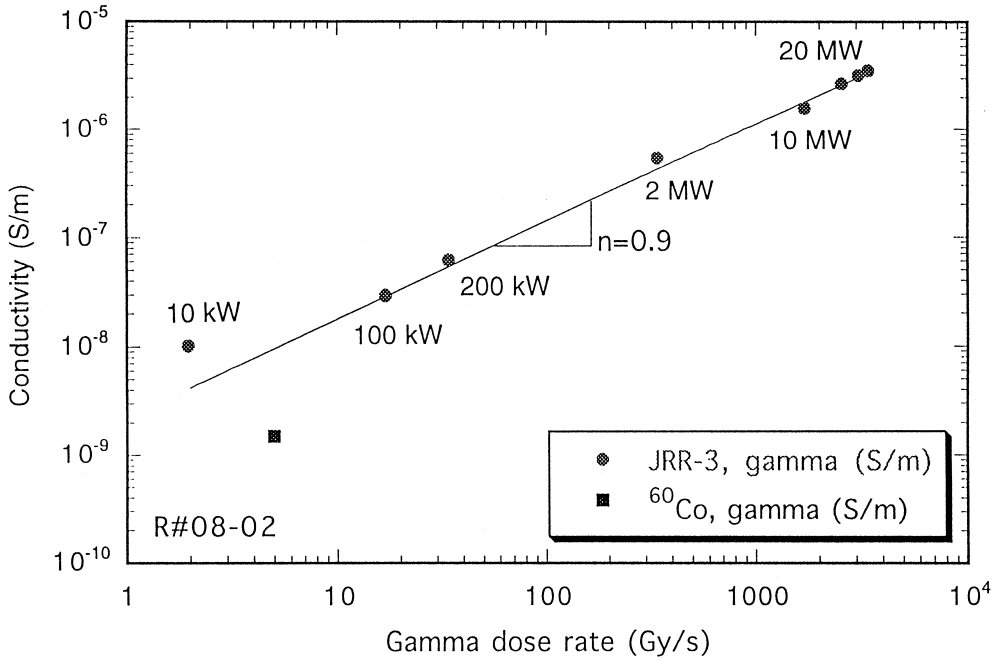

Fig. 9. Conductivity calculated for the Al_2O_3 specimen as a function of the gamma-ray dose rate evaluated from the reactor power.

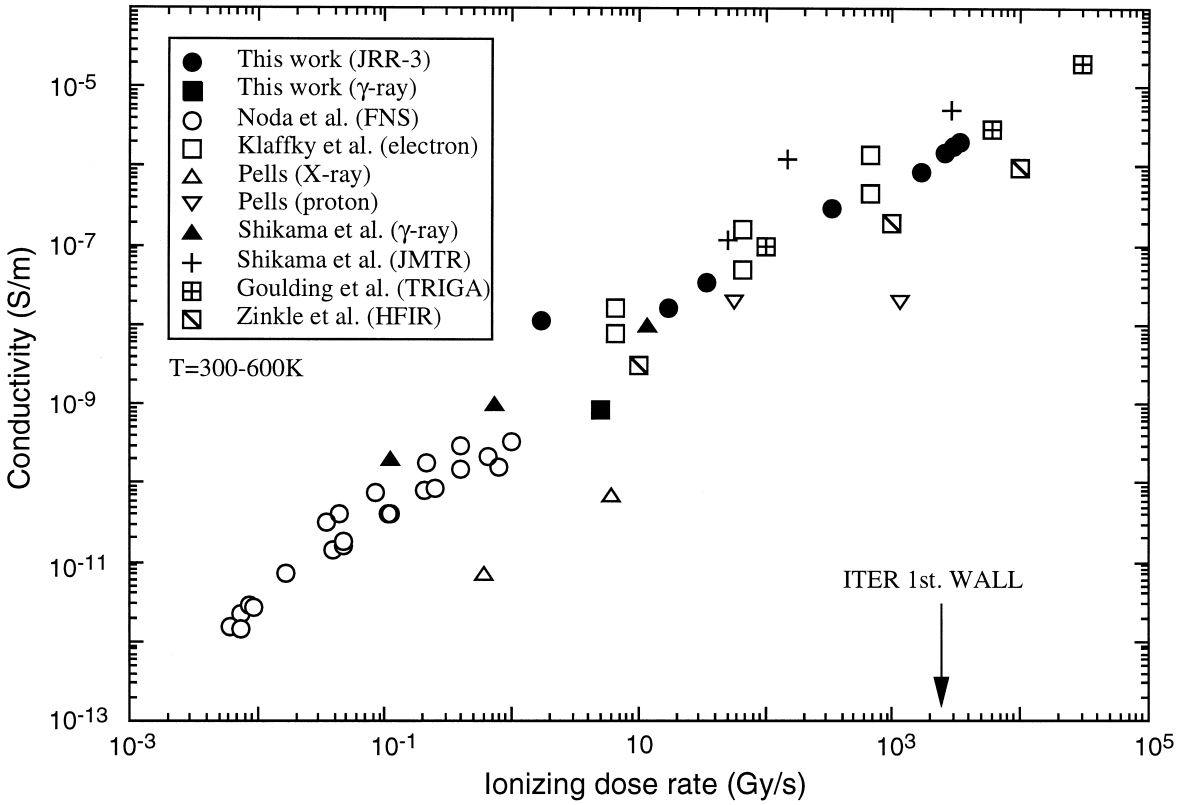

Fig. 10. Comparison between the ionizing dose rate dependence of the conductivity in Fig. 9 and the other RIC data of Al_2O_3.

i.e. much smaller than the gamma-ray dose rate. The gamma dose rate and the neutron flux are roughly proportional to the reactor power. As mentioned previously, the influence of leakage currents on the measured current, which would prevent the proper evaluation of the bulk conductivity of the specimen from the measured current, should be small for the center current in comparison with the HV source current. The electrical conductivity was evaluated from the center current for the Al_2O_3 specimen, for which the center current was measured with the increase of the reactor power after the reactor operation start in the first irradiation cycle shown in Fig. 4. The conductivity calculated for the Al_2O_3 specimen is shown as a function of the gamma-ray dose rate evaluated from the rector power in Fig. 9. The conductivity increased with the gamma-ray dose rate and increase of the conductivity with the irradiation fluence was not observed up to 0.2 dpa as mentioned previously. This means that the conductivity increased with the dose rate due to RIC, but no evidence for RIED was observed. The gamma-ray dose rate dependence of the conductivity has the gradient of about 1 in a log–log plot and is consistent with (somewhat higher than) the conductivity of the Al_2O_3 specimen which was measured under the ^{60}Co gamma-ray irradiation (5 Gy/s, 573 K) in the present study. Although the temperature of the specimen was raised from room temperature to 540 K due to increase of the reactor power, such conductivity dominantly depends on the gamma dose rate rather than temperature as shown in Fig. 9. The increase of conductivity due to RIC arising from an increase of ionizing dose rate has been shown to be much larger than the temperature dependence of the conductivity in this temperature range, according to gamma-ray, electron and 14 MeV neutron irradiation studies on high-purity Al_2O_3 [4,8,21,22]

Fig. 10 shows a comparison between the ionizing dose rate dependence of the conductivity in Fig. 9 and the other RIC data on Al_2O_3 including the data for the same kinds of Al_2O_3 (Kyocera SA 100) in the studies of Shikama et al. [11]. The conductivity values estimated in the present study fall within the data scatter band of previous studies [3,4,8,10,11,21–23], although they are larger than the data in some studies such as the recent work using HFIR by about one order of magnitude. This seems to suggest that the center current measurement was a reasonably accurate estimator of bulk conductivity of the specimens.

Acknowledgements

The authors wish to express their thanks to Dr H. Katsuta and Dr H. Nakajima for their interests in this

work. The authors are also indebted to technical cooperation of specialists of the Research Reactor Utilization Division for preparation of the irradiation capsule.

References

[1] S.J. Zinkle, E.R. Hodgson, J. Nucl. Mater. 191–194 (1992) 58.
[2] L.W. Hobbs, F.W. Clinard Jr., S.J. Zinkle, R.C. Ewing, J. Nucl. Mater. 216 (1994) 291.
[3] R.W. Klaffky, B.H. Rose, A.N. Goland, G.J. Dienes, Phys. Rev. B 21 (1980) 3610.
[4] G.P. Pells, Radiat. Eff. 97 (1986) 199.
[5] E.R. Hodgson, S. Clement, J. Nucl. Mater. 155–157 (1988) 357.
[6] T. Shikama, M. Narui, Y. Endo, A. Ochiai, H. Kayano, J. Nucl. Mater. 191–194 (1992) 544.
[7] H. Bock, M. Suleiman, Nucl. Instrum. Meth. 148 (1978) 43.
[8] K. Noda, T. Nakazawa, Y. Oyama, H. Maekawa, J. Kaneda, C. Kinoshita, Fusion Eng. Des. 29 (1995) 448.
[9] E.R. Hodgson, J. Nucl. Mater. 179–181 (1991) 383.
[10] G.P. Pells, J. Nucl. Mater. 184 (1991) 177.
[11] T. Shikama, M. Narui, Y. Endo, T. Sagawa, H. Kayano, J. Nucl. Mater. 191–194 (1992) 575.
[12] A. Moeslang, E. Daum, R. Lindau, Proc. 18th Symp. on Fusion Tech. Karlsruhe, Germany, Aug. 22–26, 1994, p. 1313.
[13] X.F. Zong, C.F. Shen, S. Liu, Z.C. Wu, Yi. Chen, Y. Chen, B.D. Evans, R. Gonzalez, C.H. Sellers, Phys. Rev. B 49 (1994) 15514.
[14] C. Pathuwathavithane, W.Y. Wu, R.H. Zee, J. Nucl. Mater. 225 (1995) 328.
[15] W. Kesternich, F. Scheuermann, S.J. Zinkle, J. Nucl. Mater. 219 (1995) 190.
[16] L.L. Snead, D.P. White, S.J. Zinkle, J. Nucl. Mater. 226 (1995) 58.
[17] E.H. Farnum, T. Shikama, M. Narui, T. Sagawa, K. Scarborough, J. Nucl. Mater. 228 (1996) 117.
[18] G.P. Pells, E.R. Hodgson, J. Nucl. Mater. 226 (1995) 286.
[19] S.J. Zinkle, J.D. Hunn, R.E. Stoller, Mater. Res. Soc. Symp. Proc., vol. 373, Material Research Society, Pittsburg, PA, 1995, p. 299.
[20] Y. Katano, K. Nakata, S. Kasahara, H. Ohno, J. Nucl. Mater. 191–194 (1992) 598.
[21] K. Shiiyama, T. Izu, C. Kinoshita, M. Kutuwada, J. Nucl. Mater. 233–237 (1996) 1332.
[22] S.J. Zinkle, D.P. White, L.L. Snead, W.S. Eatherly, A.L. Qualls, D.W. Heatherly, R.G. Sitterson, R.L. Wallace, D.G. Raby, M.T. Hurst, E.H. Farnum, K. Scarborough, T. Shikama, M. Narui, K. Shiiyama, Fusion Material Semiann. Prog. Report for the period ending June 30, 1996, DOE/ER-0313/20, p. 257.
[23] R.H. Goulding, S.J. Zinkle, D.A. Rasmussen, R.E. Stoller, J. Appl. Phys. 79 (1996) 2920.